



Published in final edited form as:

Oral Oncol. 2013 January ; 49(1): 15–19. doi:10.1016/j.oraloncology.2012.07.017.

Near-Infrared Fluorescence Sentinel Lymph Node Mapping of the Oral Cavity in Head and Neck Cancer Patients

Joost R. van der Vorst, M.D.¹, Boudewijn E. Schaafsma, M.D.¹, Floris P.R. Verbeek¹, Stijn Keereweer, M.D.⁴, Jeroen C. Jansen, M.D., Ph.D.², Lilly-Ann van der Velden, M.D., Ph.D.², Antonius Langeveld, M.D., Ph.D.², Merlijn Hutteman, Ph.D.¹, Clemens Löwik, Ph.D.³, Cornelis J.H. van de Velde, M.D., Ph.D.¹, John V. Frangioni, M.D., Ph.D.^{5,6}, and Alexander L. Vahrmeijer, M.D., Ph.D.¹

¹Department of Surgery, Leiden University Medical Center, Leiden, the Netherlands ²Department of Otolaryngology and Head & Neck Surgery, Leiden University Medical Center, Leiden, the Netherlands ³Department of Endocrinology, Leiden University Medical Center, Leiden, the Netherlands ⁴Department of Otorhinolaryngology Head and Neck Surgery, Erasmus Medical Center, Rotterdam, the Netherlands ⁵Department of Radiology, Beth Israel Deaconess Medical Center, Boston, MA 02215 ⁶Division of Hematology/Oncology, Department of Medicine, Beth Israel Deaconess Medical Center, Boston, MA 02215

Abstract

Objectives—Elective neck dissection is frequently performed during surgery in head and neck cancer patients. The sentinel lymph node (SLN) procedure can prevent the morbidity of a neck dissection and improve lymph node staging by fine pathology. Near-infrared (NIR) fluorescence imaging is a promising technique to identify the sentinel lymph node (SLN) intraoperatively. This feasibility study explored the use of indocyanine green adsorbed to human serum albumin (ICG:HSA) for SLN mapping in head and neck cancer patients.

Materials and Methods—A total of 10 consecutive patients with oral cavity or oropharyngeal cancer and a clinical N0 neck were included. After exposure of the neck, 1.6 mL of ICG:HSA (500 μ M) was injected at 4 quadrants around the tumor. During the neck dissection, levels I, II, III and IV were measured for fluorescence using the Mini-FLARE imaging system.

Results—In all 10 patients, NIR fluorescence imaging enabled visualization of one or more SLNs. A total of 17 SLNs were identified. The mean contrast between the fluorescent signal of the lymph nodes and of the surrounding tissue was 8.7 ± 6.4 . In 3 patients, of which 1 was false-negative, lymph node metastases were found. After administration of ICG:HSA, the average number of fluorescent lymph nodes significantly increased over time ($P < 0.001$).

Conclusion—This study demonstrated feasibility to detect draining lymph nodes in head and neck cancer patients using NIR fluorescence imaging. However, the fluorescent tracer quickly migrated beyond the SLN to higher tier nodes.

Keywords

Near-Infrared Fluorescence; Image-Guided Surgery; Oral Cavity Cancer; Oropharynx Cancer; Sentinel Lymph Node; Indocyanine Green

INTRODUCTION

In head and neck cancer patients, cervical lymph node involvement is the single most important prognostic factor.^{1,2} To obtain adequate staging and local control of the cervical region, elective neck dissections are frequently performed, even in patients with clinical and radiological N0 stage. In approximately 25% of these patients, lymph node metastases are found.³ Furthermore, micrometastases and isolated tumor cells are often missed during standard pathological workup.

To decrease the morbidity of neck dissection and to improve lymph node staging by fine pathology, the sentinel lymph node (SLN) procedure has been advocated. The SLN procedure is based on the theory that flow from a tumor travels sequentially to the first tier node (i.e. the sentinel node) and subsequently to the remaining lymph node basin. The SLN procedure is currently standard of care in breast cancer and melanoma in most centers. Although much work has been performed in head and neck cancer, the SLN procedure has not yet been established as standard of care.⁴⁻⁷ As in breast cancer, the use of radiocolloids and a blue dye can be considered the gold standard to locate the SLN. However, the disadvantages of radiocolloids are the lack of real-time intraoperative visual information and the need for a nuclear physician; and disadvantages of blue dyes include limited depth penetration and blue staining of the surgical field.

Recently, the use of near-infrared (NIR) fluorescent light has been introduced to intraoperatively to identify lymph nodes, tumors and vital structures.⁸ NIR fluorescence using the fluorescent dye indocyanine green (ICG) has been successfully used for sentinel lymph node mapping in breast cancer, melanoma, cervical cancer, and vulvar cancer.⁹⁻¹² The concept of NIR fluorescence guided SLN mapping in oropharyngeal cancer has also been reported in humans.¹³ However, in the study by Bredell et al.¹³, the interval between injection of ICG and imaging varied between 5 and 30 min, which can result in identification of higher tier nodes. Preclinical work suggests that premixing ICG with human serum albumin (complex: ICG:HSA) could improve the fluorescent properties and improves retention in the SLN due to its increased hydrodynamic diameter.¹⁴ Furthermore, the injected dose of ICG (without HSA) used by Bredell et al. was 10 mg per patient. Several clinical dose-finding studies have shown that a significant lower dose (0.5–1.0 mg ICG:HSA) can successfully be used for sentinel lymph node mapping in other indications.¹⁰⁻¹² The aim of the current study was to assess the feasibility of NIR fluorescence and ICG:HSA for SLN mapping in head and neck cancer using 1.6 ml of 500 μ M ICG:HSA and the Mini-FLARE imaging system.

PATIENTS AND METHODS

Preparation of Indocyanine Green Adsorbed to Human Serum Albumin

ICG (25 mg vials) was from Pulsion Medical Systems (Munich, Germany) and was resuspended in 10 cc of sterile water for injection to yield a 2.5-mg/ml (3.2-mM) stock solution. Of this solution, 7.8 cc was transferred to a 50-cc vial of Cealb (20% human serum albumin (HSA) solution; Sanquin, Amsterdam, The Netherlands) to yield ICG in HSA (ICG:HSA) at a final concentration of 500 μ M.

Intraoperative NIR Fluorescence Imaging

SLN mapping was performed using the Mini-FLARE image-guided surgery system as described before.¹¹ Briefly, the system consists of 2 wavelength-isolated light sources: a “white” light source, generating 26,600 lx of 400 to 650-nm light and a “near-infrared” light source, generating 7.7-mW/cm² of 760-nm light. Color video and NIR fluorescence images are simultaneously acquired and displayed in real time using custom optics and software that

separate the color video and NIR fluorescence images. A pseudo-colored (lime green) merged image of the color video and NIR fluorescence images is also displayed. The imaging head is attached to a flexible gooseneck arm, which permits positioning of the imaging head virtually anywhere over the surgical field, and at extreme angles. For intraoperative use, the imaging head and imaging system pole stand are wrapped in a sterile shield and drape (Medical Technique Inc., Tucson, AZ).

Clinical Trial

The single-institution clinical trial was approved by the Medical Ethics Committee of the Leiden University Medical Center and was performed in accordance with the ethical standards of the Helsinki Declaration of 1975. A total of 10 consecutive patients with oral cavity or oropharyngeal cancer, and a clinical and radiological N0 neck were included. All patients underwent ultrasound guided cytology of lymph nodes in the neck region to assess nodal status. All patients provided informed consent and were anonymized. Exclusion criteria were pregnancy, lactation or an allergy to iodine, shellfish, or indocyanine green.

After exposure of the neck following subplatysmal flap elevation, 1.6-mL ICG:HSA (500 μ M) was injected at 4 quadrants around the tumor using a 21G, 1½ inch needle. During the neck dissection, levels I, II, III and IV were measured for fluorescence using the Mini-FLARE imaging system after injection of ICG:HSA. To assess the occurrence of drainage to higher tier nodes and the optimal time of imaging after injection, measurements were performed at 5, 10, 15, 20, 25, 30, 45 and 60 min after injection. All first draining NIR fluorescent hotspots were considered SLNs and were marked using sutures. The neck dissections consisted of resection of level I, IIa, IIb and III and in some cases level IV. The resection of the primary tumor afterwards was performed following standard procedure. Afterwards, all resected lymph nodes were examined by routine histopathological analysis; lymph nodes were fixed in formalin and embedded in paraffin for routine hematoxylin and eosin staining. SLNs and non-SLNs were examined separately.

Statistical Analysis

For statistical analysis and to generate graphs, GraphPad Prism Software (Version 5.01, La Jolla, CA) was used. Age, body mass index (BMI) and tumor size were reported as median and range. Signal-to-background ratio (SBR) was reported as mean and standard deviation. Difference in number of lymph nodes identified between time points was tested using a repeated measures ANOVA.

RESULTS

Patient and Tumor Characteristics

Patient and tumor characteristics are detailed in Table 1. Ten patients with oral cavity or oropharyngeal tumors and a clinical and radiological stage N0 were included. Median patient age was 59.5 years (range 33–73 years), median BMI was 24 (range 19–35 kg/m²), and median primary tumor size was 2.2 cm (range 0.3–5.2 cm). Location of primary tumor was the tongue in 7 patients, tonsil region in 2 patients, and retromolar trigone in 1 patient. Four patients underwent a hemiglossectomy, 4 patients underwent a commando resection, and 2 patients underwent a pull-through resection. Nine patients underwent a unilateral neck dissection and 1 patient a bilateral neck dissection. One patient was previously treated for a laryngeal cancer and developed a second primary tumor after a disease-free period of 10 y, for which the patient was treated and included in the current study. This patient was initially treated with surgical removal of the tumor and bilateral radiotherapy of the neck region. After histological examination, 9 patients were diagnosed with a squamous cell carcinoma and 1 patient with a basal cell adenocarcinoma.

Intraoperative NIR Fluorescence Imaging

In all patients (N = 10), NIR fluorescence imaging enabled identification of 1 or more SLNs. An example of the intraoperative identification of a SLN using NIR fluorescence is shown in Figure 1. A total of 17 SLNs were detected. On average, 1.7 ± 0.8 SLNs per patient were detected and a total of 22.9 ± 9.7 lymph nodes were resected per patient (Table 2). The average contrast between fluorescent signal of the SLN and the surrounding tissue was 8.7 ± 6.4 . In 3 patients, the identified SLNs were located in level I, in 5 patients in level IIA and in 2 patients in level III. No adverse reactions or complications occurred during the current study. Histological analysis showed that 3 out of 10 patients had metastatic disease, all in a single lymph node. In 2 cases, the tumor-positive lymph node was the NIR fluorescent SLN, and in 1 patient the tumor-positive lymph node was a non-SLN located in level 2A, which was also not NIR fluorescent. No adverse reactions occurred.

Intraoperative lymphatic mapping

To assess the occurrence of drainage to higher tier nodes and the optimal time of imaging after injection, NIR fluorescence was measured at several time points after injection (Fig. 2). All first draining NIR fluorescent hotspots were considered SLNs and were marked using sutures. Additional lymph nodes that became fluorescent during later imaging time-points were allocated as higher tier non-SLNs. In 7 of 10 patients SLNs could be identified within 5 min after injection. In 3 patients, SLNs were detected after 10, 15 and 30 min, respectively. Using a repeated measures ANOVA test, the average number of fluorescent lymph nodes significantly increased over time ($P < 0.001$; Fig. 3; Table 3).

DISCUSSION

The current study examined the feasibility of using the Mini-FLARE imaging system and ICG:HSA for intraoperative fluorescence guided SLN mapping in head and neck cancer patients. In all patients, 1 or more SLNs could be identified during surgery, and in the majority of patients the SLN could be identified within 5 min after injection. The average contrast between fluorescence of the SLNs and background fluorescence was 8.7, which is consistent with SBRs that were reported for fluorescence SLN mapping studies using ICG:HSA in other cancer types.⁹⁻¹¹ Another important finding of the current study was that after several min, ICG:HSA drains to second tier nodes, which can possibly result in the identification of false-positive sentinel nodes.

Bredell et al. was the first to describe the successful use of NIR fluorescence in SLN mapping in oropharyngeal cancer patients. In this study, the time between injection of ICG (without HSA) and imaging varied between 5 and 30 min. Based on the present study, this could result in identification of higher tier lymph nodes. Furthermore, the injected dose of ICG used in the previous study was 10 mg, which is considerably higher than the dose used in the present study (0.62 mg). In breast cancer patients, our group has shown that when ICG is injected in a high dose, a phenomenon known as quenching can occur, which can result in a decrease of the NIR fluorescence signal.¹¹

Based on previous preclinical results, ICG was premixed with HSA in the current study to obtain better retention in the SLN and to increase quantum yield.¹⁴ However, it still remains unclear if premixing ICG with HSA is necessary or significantly improves performance. A randomized clinical trial in breast cancer patients reported no differences between using ICG:HSA and ICG alone.⁹ However, the effect of premixing ICG with HSA is potentially indication-specific, therefore this should be examined for head and neck cancer patients. The SLN procedure in breast cancer patients does not allow assessment of flow to higher echelon lymph nodes. Therefore, the present study in which patients underwent a neck dissection

creates an ideal platform to assess the degree and rate of flow to higher echelon nodes. As we showed in Table 3, a high degree of flow to higher echelon lymph nodes was observed since the average number of fluorescent lymph nodes identified an hour after administration of ICG:HSA was 6.1 ± 3.5 , which was significantly higher than the average number of SLNs of 1.7 ± 0.8 .

Another approach recently presented by van der Poel et al. is combining fluorescence and radioactivity in 1 lymphatic tracer by simply premixing ^{99m}Tc -NanoColl and ICG.¹⁵ Using this multimodal tracer injected by the nuclear physician before surgery, time of surgery will probably be shortened because the dye does not have to be injected during surgery. Furthermore, preoperative SLN localization and subsequent surgical planning can be performed using a lymphoscintigraphy or a SPECT/CT exam. Heuveling et al. demonstrated SLN mapping in rabbits using Nanocolloidal albumin which was covalently conjugated to IRDye-800CW, which showed excellent retention in the SLN after 24 hr.¹⁶ However, translation of this compound to a clinical setting remains challenging due to regulatory issues.

The current study showed a relatively wide range in time between injection of ICG:HSA and identification of the SLN, which was 30 min in 1 patient. This particular patient was treated for a primary laryngeal tumor by resection and cervical radiotherapy 10 y prior to the current study, and only 1 fluorescent lymph node could be detected. After pathological workup, 15 lymph nodes were detected. Radiation can influence microvasculature and damage the capillary network, which manifests itself as telangiectatic vessels that increase over time.¹⁷ Other studies showed that repair of damaged endothelium by angiogenesis is inhibited by radiotherapy.¹⁸ Similar damage and aberrant repair may occur in lymphatic microvessels after radiation. Therefore, a possible explanation for the relatively long time to identify the SLN in this patient was that damage to the lymphatic microvessels perturbed drainage in the irradiated neck. Furthermore, it is known from rectal cancer studies that an average of approximately 5 times fewer nodes can be identified in resection specimens when patients are treated with neoadjuvant radiation compared to patients only treated with surgery.¹⁹ When translating these results to head and neck cancer patients, prudence should be applied in patients pretreated with radiation since SLN mapping can be more challenging in these patients.

Based on standard pathology, in 1 of 3 patients with positive nodes, tumor cells were detected in a non-SLN, while the SLNs did not contain tumor. The reason for this patient being false-negatively staged remains unclear. A potential explanation could be that in case of multiple drainage patterns, a subset of SLNs can become fluorescent later, and will be incorrectly identified as higher tier lymph nodes. Future research should therefore be focused on fluorescent tracers that are retained in the first draining node(s), which makes it possible to perform imaging later after injection of the dye. Furthermore, the relatively low depth sensitivity of the current generation imaging systems (on the order of millimeters), could be an explanation for false-negative results. Another potential explanation could be the occurrence of a skip metastasis in this particular patient, which has been reported previously in head and neck cancer patients.²⁰ Since only 10 patients were included in the current study, a final potential explanation for this patient being false-negative is the learning curve associated with tracer injection and imaging. Therefore, the false-negative rate has to be assessed in larger patient series.

In conclusion, the current study successfully showed the use of NIR fluorescence and ICG:HSA for intraoperative identification of the SLN in oropharynx and oral cavity cancer patients. Optimal dosage, true false-negative rate, and optimization of lymphatic tracers and possibly multimodal hybrid tracers, are topics for future studies.

Acknowledgments

The authors thank Lindsey Gendall for editing. This work was supported in part by the Dutch Cancer Society grant UL2010-4732 and National Institutes of Health grant R01-CA-115296. This work was supported in part by the Center of Translational Molecular Medicine (MUSIS project, grant 03O-202-04).

References

1. Leemans CR, Tiwari R, Nauta JJ, van dW I, Snow GB. Regional lymph node involvement and its significance in the development of distant metastases in head and neck carcinoma. *Cancer*. 1993; 71:452–456. [PubMed: 8422638]
2. Layland MK, Sessions DG, Lenox J. The influence of lymph node metastasis in the treatment of squamous cell carcinoma of the oral cavity, oropharynx, larynx, and hypopharynx: N0 versus N+ Laryngoscope. 2005; 115:629–639. [PubMed: 15805872]
3. Sheahan P, O'Keane C, Sheahan JN, O'Dwyer TP. Effect of tumour thickness and other factors on the risk of regional disease and treatment of the N0 neck in early oral squamous carcinoma. *Clin Otolaryngol Allied Sci*. 2003; 28:461–471. [PubMed: 12969352]
4. Alkureishi LW, Ross GL, Shoaib T, Soutar DS, Robertson AG, Thompson R, et al. Sentinel node biopsy in head and neck squamous cell cancer: 5-year follow-up of a European multicenter trial. *Ann Surg Oncol*. 2010; 17:2459–2464. [PubMed: 20552410]
5. Burcia V, Costes V, Faillie JL, Gardiner Q, de VD, Cartier C, et al. Neck restaging with sentinel node biopsy in T1-T2N0 oral and oropharyngeal cancer: Why and how? *Otolaryngol Head Neck Surg*. 2010; 142:592–597. [PubMed: 20304284]
6. Civantos FJ, Zitsch RP, Schuller DE, Agrawal A, Smith RB, Nason R, et al. Sentinel lymph node biopsy accurately stages the regional lymph nodes for T1-T2 oral squamous cell carcinomas: results of a prospective multi-institutional trial. *J Clin Oncol*. 2010; 28:1395–1400. [PubMed: 20142602]
7. Kuriakose MA, Trivedi NP. Sentinel node biopsy in head and neck squamous cell carcinoma. *Curr Opin Otolaryngol Head Neck Surg*. 2009; 17:100–110. [PubMed: 19337128]
8. Schaafsma BE, Mieog JS, Hutteman M, van der Vorst JR, Kuppen PJ, Lowik CW, et al. The clinical use of indocyanine green as a near-infrared fluorescent contrast agent for image-guided oncologic surgery. *J Surg Oncol*. 2011; 104:323–332. [PubMed: 21495033]
9. Hutteman M, Mieog JS, van der Vorst JR, Liefers GJ, Putter H, Lowik CW, et al. Randomized, double-blind comparison of indocyanine green with or without albumin premixing for near-infrared fluorescence imaging of sentinel lymph nodes in breast cancer patients. *Breast Cancer Res Treat*. 2011; 127:163–170. [PubMed: 21360075]
10. Hutteman M, van der Vorst JR, Gaarenstroom KN, Peters AA, Mieog JS, Schaafsma BE, et al. Optimization of near-infrared fluorescent sentinel lymph node mapping for vulvar cancer. *Am J Obstet Gynecol*. 2011
11. Mieog JS, Troyan SL, Hutteman M, Donohoe KJ, van der Vorst JR, Stockdale A, et al. Toward Optimization of Imaging System and Lymphatic Tracer for Near-Infrared Fluorescent Sentinel Lymph Node Mapping in Breast Cancer. *Ann Surg Oncol*. 2011
12. van der Vorst JR, Hutteman M, Gaarenstroom KN, Peters AA, Mieog JS, Schaafsma BE, et al. Optimization of near-infrared fluorescent sentinel lymph node mapping in cervical cancer patients. *Int J Gynecol Cancer*. 2011; 21:1472–1478. [PubMed: 22027751]
13. Bredell MG. Sentinel lymph node mapping by indocyanin green fluorescence imaging in oropharyngeal cancer - preliminary experience. *Head Neck Oncol*. 2010; 2:31. [PubMed: 21034503]
14. Ohnishi S, Lomnes SJ, Laurence RG, Gogbashian A, Mariani G, Frangioni JV. Organic alternatives to quantum dots for intraoperative near-infrared fluorescent sentinel lymph node mapping. *Mol Imaging*. 2005; 4:172–181. [PubMed: 16194449]
15. van der Poel HG, Buckle T, Brouwer OR, Valdes Olmos RA, van Leeuwen FW. Intraoperative Laparoscopic Fluorescence Guidance to the Sentinel Lymph Node in Prostate Cancer Patients: Clinical Proof of Concept of an Integrated Functional Imaging Approach Using a Multimodal Tracer. *Eur Urol*. 2011

16. Heuveling DA, Visser GW, de GM, de Boer JF, Baclayon M, Roos WH, et al. Nanocolloidal albumin-IRDye 800CW: a near-infrared fluorescent tracer with optimal retention in the sentinel lymph node. *Eur J Nucl Med Mol Imaging*. 2012
17. Turesson I. Individual variation and dose dependency in the progression rate of skin telangiectasia. *Int J Radiat Oncol Biol Phys*. 1990; 19:1569–1574. [PubMed: 2262383]
18. Scharpfenecker M, Kruse JJ, Sprong D, Russell NS, Ten DP, Stewart FA. Ionizing radiation shifts the PAI-1/ID-1 balance and activates notch signaling in endothelial cells. *Int J Radiat Oncol Biol Phys*. 2009; 73:506–513. [PubMed: 19147015]
19. Govindarajan A, Gonen M, Weiser MR, Shia J, Temple LK, Guillem JG, et al. Challenging the feasibility and clinical significance of current guidelines on lymph node examination in rectal cancer in the era of neoadjuvant therapy. *J Clin Oncol*. 2011; 29:4568–4573. [PubMed: 21990400]
20. Lodder WL, Sewnaik A, den Bakker MA, Meeuwis CA, Kerrebijn JD. Selective neck dissection for N0 and N1 oral cavity and oropharyngeal cancer: are skip metastases a real danger? *Clin Otolaryngol*. 2008; 33:450–457. [PubMed: 18983378]

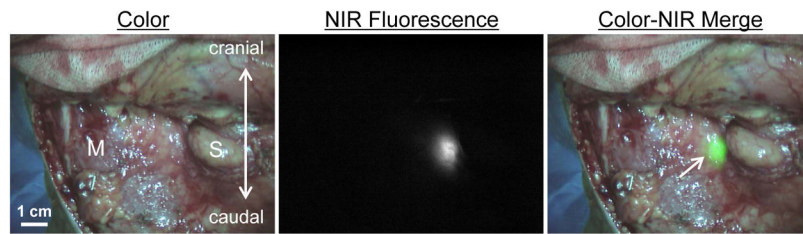


Figure 1. Sentinel lymph node mapping using NIR fluorescence imaging in oropharyngeal cancer patients

Peritumoral injection of 1.6 mL of 500- μ M ICG:HSA identifies a SLN (arrow) in an oropharyngeal cancer patient. M = sternocleidomastoid muscle and S = submandibular gland.

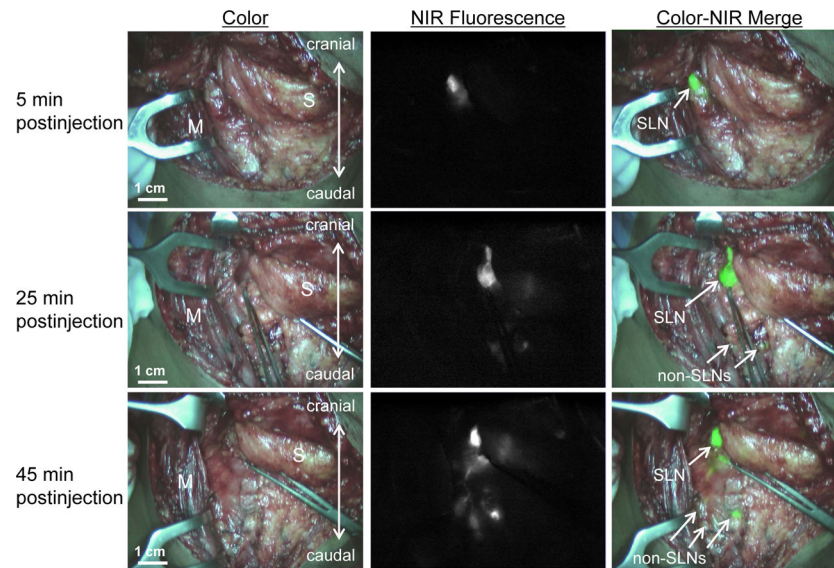


Figure 2. Sentinel lymph node mapping in head and neck cancer over time

One SLN (arrows) can be clearly identified 5 min (top row) postinjection of 1.6 mL of 500- μ M ICG:HSA around the primary tumor. Identification of higher tier nodes was observed after 25 min (middle row), and the number of fluorescent lymph nodes increased further at 45 min postinjection (bottom row). M = sternocleidomastoid muscle and S = submandibular gland.

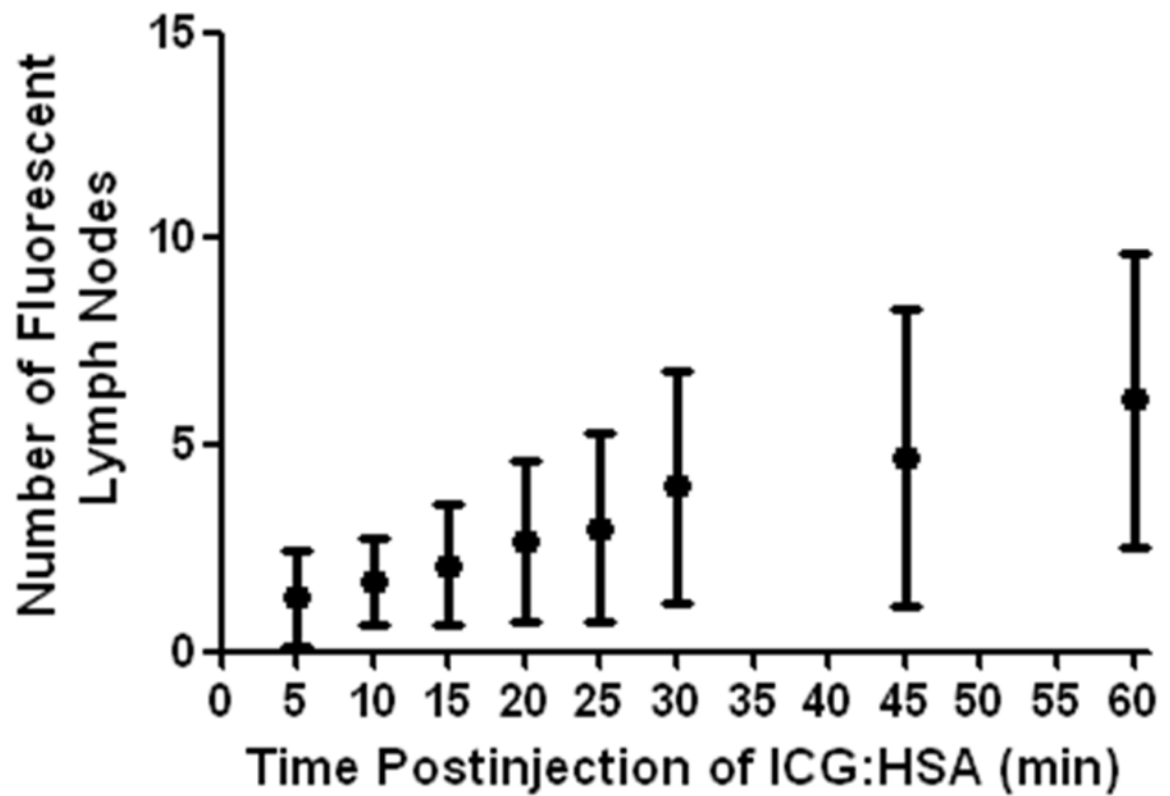


Figure 3. Lymph node identification as a function of postinjection time
Number of fluorescent lymph nodes (mean \pm S.D.) is plotted as a function of time after injection of 500- μ M ICG:HSA. The number of fluorescent lymph nodes significantly increased over time ($P < 0.001$)

Table 1

Patient and Tumor Characteristics

Patient no.	Age (Years)	BMI (kg/m ²)	Tumor Location	Type of Surgery	Tumor Type	Tumor Size (cm)
1	33	22	Tongue	Hemiglossectomy	Squamous	1.7
2	73	25	Tongue	Hemiglossectomy	Squamous	5.2
3	64	24	Oropharynx	Commando resection	Basal cell adenocarcinoma	1.3
4	62	22	Tongue	Hemiglossectomy	Squamous	3.3
5	58	23	Trigonum Retromolare	Commando resection	Squamous	0.3
6	55	27	Tongue	Hemiglossectomy	Squamous	1.6
7	52	32	Tongue	Hemiglossectomy	Squamous	3
8	63	35	Oropharynx	Commando resection	Squamous	4
9	53	24	Tongue	Pull through resection	Squamous	2.4
10	61	19	Tongue	Pull through resection	Squamous	2

BMI: Body Mass Index

Table 2

Results from *In Vivo* SLN Imaging

Patient no.	NIR Hotspots	Total LNs Harvested	LN+	Mean SBR	Location of NIR Hotspots
1	3	14	No	16.3	2A
2	1	26	No	21.0	1
3	1	30	No	12.0	1
4	3	35	Yes (SLN +)	3.2	1
5	2	9	No	2.6	2A
6	1	20	Yes (SLN +)	4.2	2A
7	2	24	No	5.2	3
8	1	15	No	4.2	3
9	2	17	Yes (SLN -)	5.7	2A
10	1	39	No	12.3	2A

NIR: Near Infrared, LN: Lymph Node, SBR: Signal-to-background

Table 3

Number of Identified NIR Fluorescent Hotspots over Time

Patient no.	NIR LNs after 5 min	NIR LNs after 10 min	NIR LNs after 15 min	NIR LNs after 20 min	NIR LNs after 25 min	NIR LNs after 30 min	NIR LNs after 45 min	NIR LNs after 60 min
1	3	3	5	7	7	8	11	11
2	1	2	2	4	4	6	9	9
3	1	2	2	2	2	2	2	2
4	3	3	3	4	4	4	4	7
5	2	2	2	2	2	2	3	8
6	0	0	1	1	1	1	1	2
7	2	2	3	3	6	9	9	9
8	0	0	0	0	0	1	1	1
9	0	2	2	2	2	3	3	8
10	1	1	1	2	3	4	4	4

NIR: Near Infrared, LN: lymph node